Article

Laccase Inhibition by As3+/As5+: Determination of Inhibition Mechanism and Preliminary Application to a Self-Powered Biosensor

Tao Wang, Ross D. Milton, Sofiene Abdellaoui, David P. Hickey, and Shelley D. Minteer

Anal. Chem., **Just Accepted Manuscript** • DOI: 10.1021/acs.analchem.5b04651 • Publication Date (Web): 11 Feb 2016

Laccase Inhibition by $As^{3+/}As^{5+}$: Determination of Inhibition Mechanism and Preliminary Application to a Self-Powered Biosensor

Tao Wang, Ross D. Milton, Sofiene Abdellaoui, David P. Hickey and Shelley D. Minteer *

Departments of Chemistry and Materials Science and Engineering, University of Utah, 315 S 1400 E Room 2020, Salt Lake City, UT, 84112, USA. E-mail: minteer@chem.utah.edu.

ABSTRACT: The reversible inhibition of laccase by arsenite (As^{3+}) and arsenate (As^{5+}) is reported for the first time. Oxygen-reducing laccase bioelectrodes were found to be inhibited by both arsenic species for direct electron transfer bioelectrodes (using anthracene functionalities for enzymatic orientation) and for mediated electron transfer bioelectrodes (using ABTS as an electron mediator). Both arsenic species were determined to behave *via* a mixed inhibition model (behaving closely to that of uncompetitive inhibitors) when evaluated spectrophotometrically using ABTS as the electron donor. Finally, laccase bioelectrodes were employed within an enzymatic fuel cell, yielding a self-powered biosensor for arsenite and arsenate. This conceptual self-powered arsenic biosensor demonstrated LODs of 13 µM for arsenite and 132 µM for arsenate. Further, this device possessed sensitivities of 0.91 ± 0.07 mV/mM for arsenite and 0.98 ± 0.02 mV/mM for arsenate.

Arsenic is a commonly occurring groundwater pollutant largely originating from mines, industrial waste and other natural processes.[1, 2] Arsenic is present in the environment in both organic and inorganic forms. Among polluting inorganic arsenic species, arsenate and arsenite are the most common and toxic forms in groundwater,[3] therefore their environmental monitoring is necessary. Electrochemical monitoring of arsenic in water has been extensively studied and different electrochemical techniques have been evaluated for their suitability of detecting arsenic in environmental samples, such as polarography,[4, 5] and cathodic or anodic stripping voltammetry.[6, 7] Electrochemical detection techniques for arsenic have been transplanted to microarray platforms aimed at portable and field-deployable sensing purposes as opposed to high sensitivity applications (such as spectroscopic and chromatographic techniques), where portability is often troublesome.[8, 9]

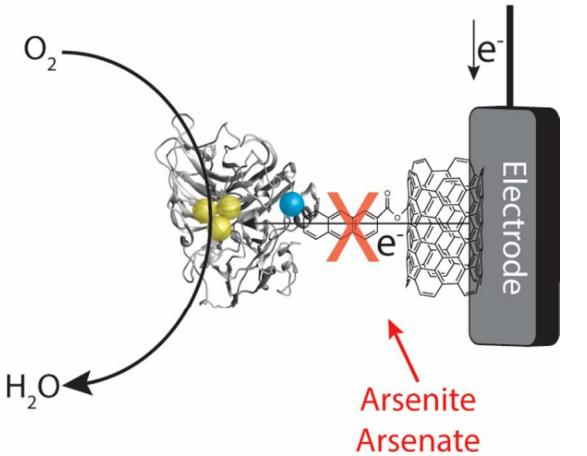

Scheme 1 – Direct electron transfer-type laccase bioelectrodes are inhibited by arsenite and arsenate.

Electrochemical arsenic sensors typically consist of a three-electrode system including a working, reference and counter electrode. A potentiostat is required to input energy into the cell and regulate the sensor. Additionally, a three-electrode device is bulky, which is unfavorable for field applications and technologies. In this paper, we aim to transition to self-powered systems for arsenic sensing.

An enzymatic fuel cell (EFC) utilizes enzymes as biocatalytic alternatives to commonly-used metal catalysts, such as platinum. EFCs are compact two-electrode systems that generate power. Self-powered biosensors based on EFC technology thus do not require an external electrical energy source.[10-22] Previous studies on self-powered biosensors have demonstrated that they are able to be fueled or inhibited by an analyte.[23-28] EFCs that are fueled by glucose have been extensively reported[29-31] and some have been extended to self-powered biosensors.[32-34] A large number of glucose/O_2 EFCs utilize laccase as the cathodic biocatalyst for O_2 reduction to H_2O.[33, 35-40] Herein, we report the first experimental evidence of the enzymatic inhibition of laccase by both arsenite and arsenate. The enzymatic inhibition model was elucidated using 2,2'-azino-bis(3-ethylbenzothiazoline-6-sulfonic acid) (ABTS) as a substrate for colorimetric assays. Further, laccase was combined with flavin adenine dinucleotide-dependent glucose dehydrogenase (FAD-GDH) to yield a glucose/O_2 EFC that is able to operate as a conceptual self-powered biosensor for arsenate and arsenite detection.

Experimental section

Chemicals and materials.

FAD-dependent glucose dehydrogenase (FAD-GDH) was purchased from Sekisui Diagnostics (UK) and used as re-

ceived. Toray carbon paper (untreated) was purchased from Fuel Cell Earth (USA) and used as received. Hydroxyl-functionalized multiwalled carbon nanotubes were purchased from Cheaptubes and used as received. Tetrabutylammonium bromide-modified Nafion (TBAB-Nafion) was prepared as previously reported.[41] All other chemicals were purchased from Sigma Aldrich (reagent grade) and used as received.

Laccase bioelectrode fabrication.

Laccase bioelectrodes are fabricated based upon a previously-published procedure: 20 mg/ml laccase in pH 5.5 citrate-phosphate buffer was mixed with 100 mg/ml anthracene-functionalized multi-walled carbon nanotubes (Ac-MWCNTs) and vortex-mixed for a total of 4 mins along with sonication for a total of 1 min.[41] The resulting mixture was then mixed with 25% v/v TBAB-Nafion, vortex-mixed for an additional minute and sonicated for an additional 15 s. Then approximately 33 µL of the mixture is applied to a 1 cm^2 square of Toray carbon paper surface via brush and dried under room temperature before evaluation.

FAD-GDH bioanode fabrication.

Dimethylferrocene-functionalized linear poly(ethylenimine) ($FeMe_2$-LPEI) was synthesized and FAD-GDH bioelectrodes were prepared, as previously reported.[42]

The FAD-GDH bioanodes were fabricated by mixing 10 mg/ml FAD-GDH, 30 mg/ml ferrocene redox polymer and 10% v/v EGDGE in a ratio of 56:24:3. A 10 µL aliquot of this mixture was applied to a 0.25 cm^2 Toray paper electrode surface and dried for 12 hr at room temperature. Electrodes were rinsed immediately before use.

UV-Vis assay for determining laccase inhibition mechanism.

UV-Vis kinetic assays were performed on a BioTex Synergy HTX multiplate reader. The absorbance of ABTS was measured at 420 nm and ABTS concentrations were: 500, 100, 40, 20, 10, 4 µM. The concentrations of arsenite and arsenate tested were 0.5, 1, 2, 4, 8, 12 mM and the concentration of laccase was 13 µg/ml. All tests were performed in citrate-phosphate buffer (200 mM pH 5.5).

Electrochemical measurements.

A conventional 3-electrode configuration was used for cyclic voltammetry and amperometric i-t experiments. A saturated calomel electrode (SCE) was used as the reference electrode and a platinum mesh was used as the counter electrode. Enzymatic fuel cells were evaluated by galvanostatically drawing increasing current from the device at a slow ramp rate (0.1 µA/s) until short circuit. The self-powered biosensor was evaluated by continuously drawing 10% of the maximum current density of the enzymatic fuel cell and monitoring the potential difference with increasing concentrations of arsenite of arsenate. All experiments were performed at 22 ± 1 ºC.

Results and discussion:

Determination of laccase inhibition reversibility.

Laccase is known to be able to undergo both mediated and direct electron transfer (MET and DET).[43-47] Laccase bioelectrodes are prepared using AcMWCNTs to orientate the type 1 copper center of laccase towards the electrode surface.[48] This favorable orientation results in DET of laccase, yielding a bioelectrode that is able to undergo the direct bioelectrocatalytic reduction of O_2 to H_2O (Figure 1).

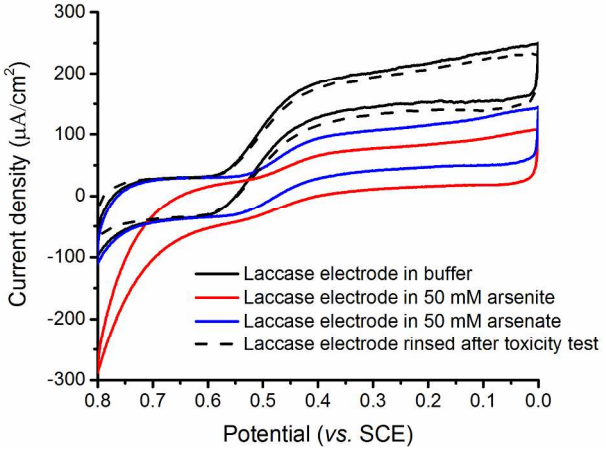

Figure 1 - Representative cyclic voltammograms of laccase bioelectrodes in citrate-phosphate buffer (200 mM, pH 5.5, stirred) in the presence of 50 mM arsenate (blue line) or 50 mM arsenite (red line). Inhibited laccase bioelectrodes were rinsed and evaluated in fresh citrate-phosphate buffer (representative dataset presented as dashed black line for As^{3+} and As^{5+} inhibited bioelectrodes). All electrodes were evaluated at a scan rate of 5 mV/s.

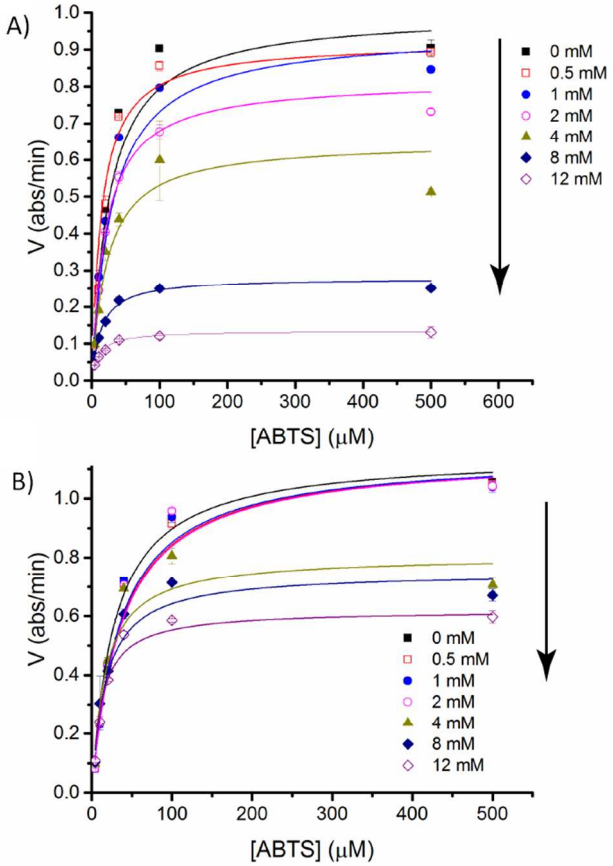

Figure 2 - Spectroscopic determination of apparent Michaelis-Menten kinetics for the oxidation of ABTS with different concentrations of A) arsenite or B) arsenate present. Kinetics were determined at pH 5.5, by following the enzymatic oxidation of ABTS at 420 nm.

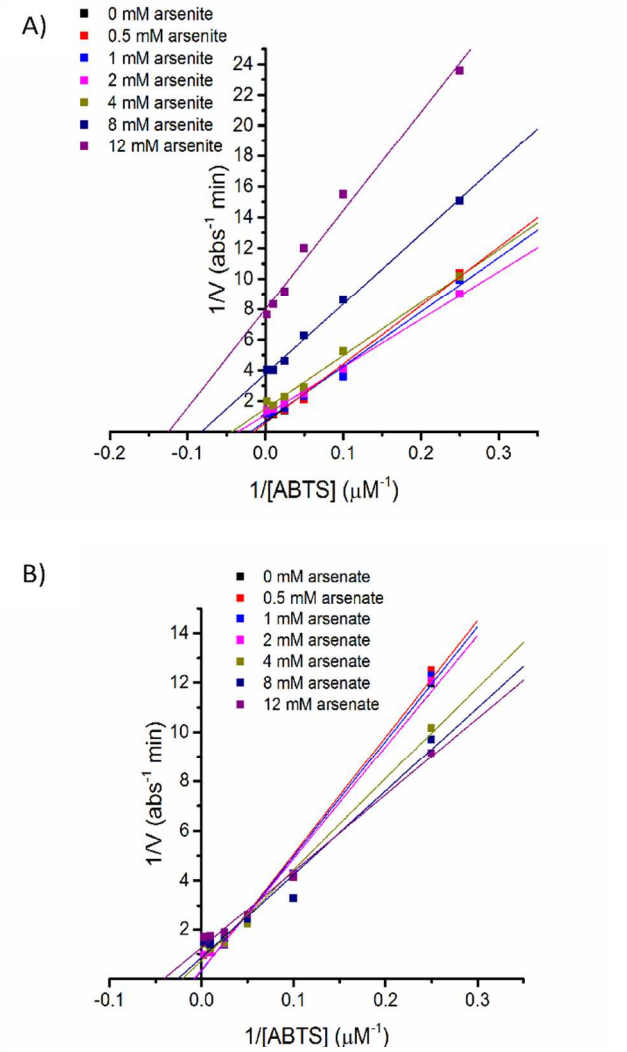

Figure 3 - Lineweaver-Burk double reciprocal plot of the reduction of O_2 by laccase, monitored by following ABTS oxidation in citrate-phosphate buffer with differing concentrations of A) arsenite and B) arsenate. Data presented as mean (n=3).

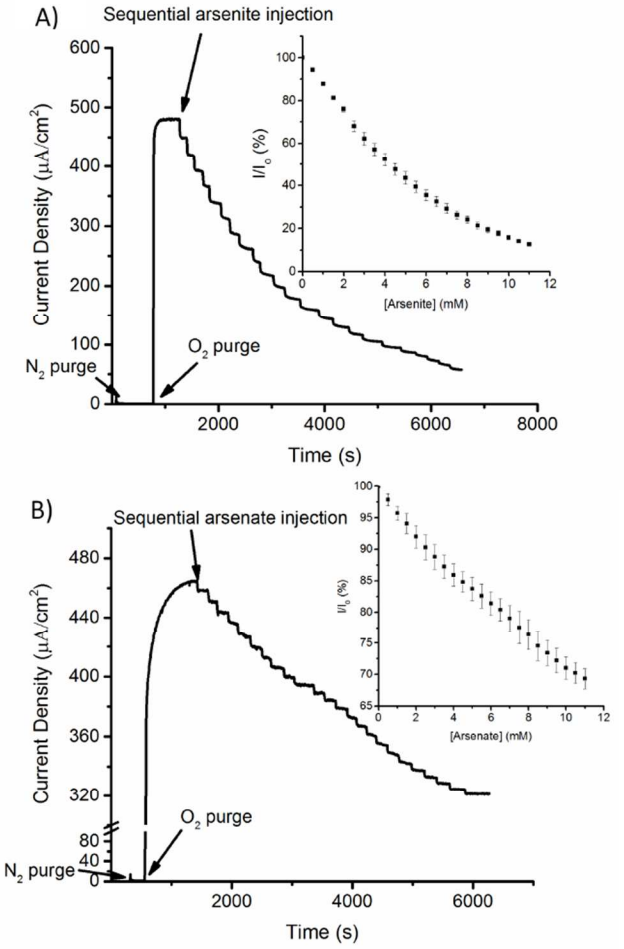

Figure 4 - Representative amperometric *i*-t curves of laccase bioelectrodes with successive injections of A) arsenite and B) arsenate. (Inset figure: Averaged percentage change of each laccase electrode with injections of A) arsenite and B) arsenate). Experiments were performed at pH 5.5 (200 mM citrate-phosphate buffer), under hydrodynamic (stirred) conditions.

The reversibility of arsenic inhibition to laccase was first investigated by evaluating laccase bioelectrodes in buffer (in the absence of arsenate or arsenite). Laccase bioelectrode that are immersed in buffer that contains dissolved O_2 results in a catalytic reductive wave, due to the direct bioelectrocatalytic reduction of O_2 to H_2O by laccase (onset potential of approximately +600 mV vs. SCE). The addition of arsenite or arsenate yields a decreased catalytic response for O_2 reduction, due to enzymatic inhibition. Replacing the buffer with arsenate/arsenite-free buffer returns the catalytic current generated by O_2 reduction to approximately 100%, demonstrating the reversibility of the inhibition mechanism.

Determination of laccase inhibition mechanism of arsenate and arsenite *via* UV-Vis colorimetric assay.

After electrochemically determining the reversibility of laccase inhibition by arsenate and arsenite, UV-Vis colorimetric assays were performed utilizing ABTS as the electron donor. An apparent rate versus arsenite and arsenate concentration is presented in Figure 2. Increasing concentrations of arsenite and arsenate (from 0 to 12 mM) result in decreasing Vmax from approximately 1.02 ± 0.08 abs/min to 0.13 ± 0.00 abs/min for arsenite and from 1.16 ± 0.06 abs/min to 0.66 ± 0.04 abs/min for arsenate (Figure 2 and Table 1). Additionally, the Michaelis constant (K_M) also decreases, which is indicative

[Arsenite]	**0 mM**	**0.5 mM**	**1 mM**	**2 mM**	**4 mM**	**8 mM**	**12 mM**
V_{max} (abs/min)	1.02 ± 0.08	0.99 ± 0.07	0.92 ± 0.04	0.78 ± 0.02	0.59 ± 0.05	0.27 ± 0.01	0.13 ± 0.0
K_M (mM)	23.2 ± 5.7	21.7 ± 4.9	21.3 ± 3.5	19.7 ± 2.1	15.8 ± 5.1	12.6 ± 1.6	10.2 ± 1.0
[Arsenate]	**0 mM**	**0.5 mM**	**1 mM**	**2 mM**	**4 mM**	**8 mM**	**12 mM**
V_{max} (abs/min)	1.16 ± 0.06	1.15 ± 0.06	1.15 ± 0.07	1.15 ± 0.07	0.93 ± 0.09	0.77 ± 0.05	0.66 ± 0.04
K_M (mM)	31.4 ± 5.2	32.6 ± 5.2	30.6 ± 5.6	30.3 ± 5.5	21.3 ± 6.4	15.6 ± 3.8	14.9 ± 2.9

Table 1 - V_{max} and K_M values of O_2 reduced by laccase monitored by following the absorbance of ABTS in citrate-phosphate buffer, the data is obtained with non-linear regression fitting.

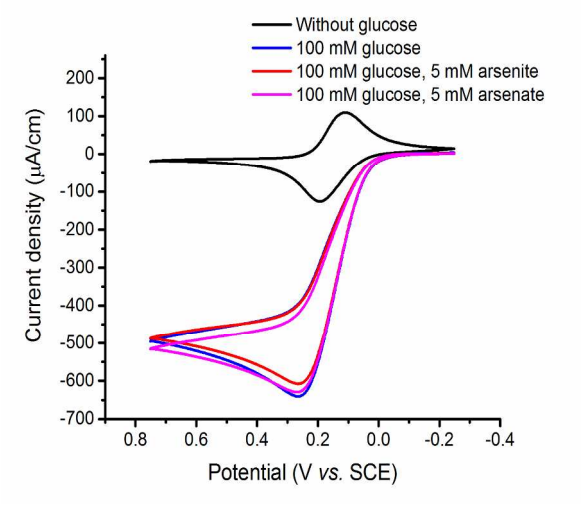

Figure 5 - Representative cyclic voltammograms of FAD-GDH bioanodes in citrate-phosphate buffer (pH 5.5, 200 mM) without glucose (black line), with 100 mM glucose (blue line), with 100 mM glucose and 5 mM arsenite (red line), and with 100 mM glucose and 5 mM arsenate (pink line). All experiments were performed at 10

of an uncompetitive inhibition mechanism.[49, 50] To further elucidate the inhibition mechanism, Lineweaver-Burk double-reciprocal plots were evaluated for differing concentrations of each inhibitor (Figure 3). A convergence of data sets on the Y-axis of Lineweaver-Burk plots is typical of a competitive inhibition mechanism, while convergence of related data sets on the X-axis is indicative of a non-competitive inhibition mechanism. Analysis of the Lineweaver-Burk double-reciprocal plots indicate a mixed inhibition model (incorporating both uncompetitive and noncompetitive inhibition models), although the nonlinear regressions performed above suggest the inhibition model lay nearer to that of an uncompetitive inhibition model. The K_i value for laccase inhibition by arsenic was determined for a mixed inhibition model (by non-linear regression), with 2.3 ± 1.4 mM reported for arsenite and 15.4 ± 10.1 mM reported for arsenate. R^2 values for individual Michaelis-Menten fittings are reported in Table 2. An uncompetitive inhibition model fit by non-linear regression yielded overall R^2 values of 0.9617 for arsenate and 0.9420 for arsenite (n = 3).

Laccase inhibition monitored by amperometry.

Subsequently, amperometric i-t analysis (Figure 4) was performed at 0.2 V (vs. SCE) with consecutive injections of either arsenate or arsenite. At this potential O_2 is reduced to H_2O by the laccase biocathodes. Following the introduction of oxygen into the nitrogen-purged buffer, a catalytic current is observed corresponding to the direct bioelectrocatalytic of reduction of oxygen by laccase. With each subsequent injection of arsenite or arsenate, a decrease in catalytic current is observed with arsenite/arsenate concentrations ranging from 0.5 to 11 mM. The corresponding catalytic currents decrease for the laccase biocathodes in the range of 5-90% current for arsenite and 2-30% current for arsenate. The laccase bioelectrodes exhibited sensitivities of 46.9 ± 7.0 μA/mM and 10.6 ± 1.2 μA/mM for

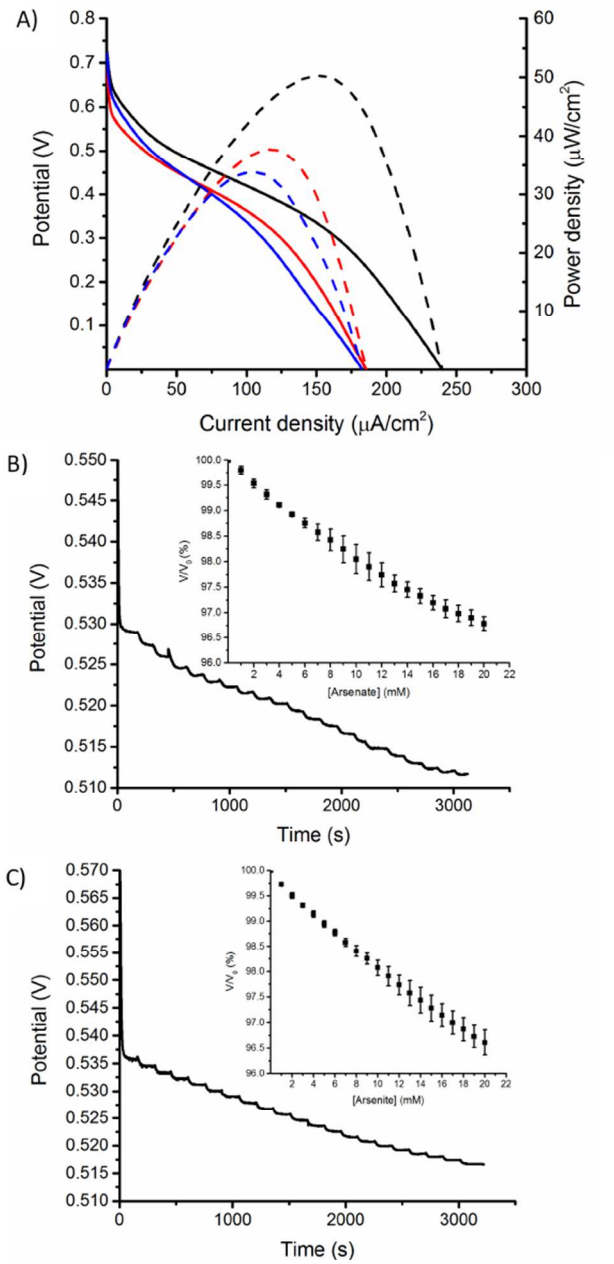

Figure 6 – A) Representative polarization curve for a glucose/O_2 EFC (black solid line), operating in citrate-phosphate buffer (pH 5.5, 200 mM, stirred) containing 100 mM glucose. Corresponding power curves are presented as dashed lines. EFCs were also operated in the presence of 20 mM arsenite (red lines) and 20 mM arsenate (blue lines). Representative chronopotentiometric traces are presented for EFCs operating at 10% current draw with sequential injections of B) 1 mM arsenite C) and 1 mM arsenate. Inset graphs present the averaged percentage change of the EFCs' potential differences with arsenic injections. Error bars represent standard deviation (n = 3 electrode pairs).

arsenite and arsenate, respectively. Their corresponding linear dynamic ranges were approximately 0.5 – 5 mM arsenite (R^2 = 0.9923) and 0.5 – 8 mM arsenate (R^2 = 0.9894).

[Arsenite]	**0**	**0.5**	**1**	**2**	**4**	**8**	**12**
R^2	0.9317	0.9635	0.9635	0.9499	0.8358	0.2593	0.9557
[Arsenate]	**0**	**0.5**	**1**	**2**	**4**	**8**	**12**
R^2	0.9787	0.9801	0.9774	0.9620	0.8710	0.9330	0.9624

Table 2- R^2 values for the non-linear regression fitting of laccase activity monitored by UV under different concentration of arsenite and arsenate

Finally, additional amperometric experiments were performed to further elucidate the enzymatic inhibition model (Supplemental Information). Laccase bioelectrodes were prepared in the absence of anthracene-functionalities on the MWCNTs (to eliminate DET contributions) and enzymatic bioelectrocatalysis was facilitated with injections of ABTS as the electron mediator and substrate (under constant O_2 concentrations) in the presence of arsenite (Figure S1 A) and arsenate (Figure S1 B). R^2 values for multiple inhibition models applied to this data by non-linear regression fits are presented in Table S1, where mixed inhibition models had the greatest correlation for both inhibitors.

Self-powered laccase arsenite and arsenate sensor.

Following the determination of the inhibition mechanism for laccase, previously-reported FAD-GDH bioanodes (incorporating a ferrocene redox polymer for MET) were coupled with laccase biocathodes (undergoing DET), yielding glucose/O_2 EFCs operating on 100 mM glucose.[42] The bioanodes and biocathodes were prepared on Toray carbon paper electrodes, with the biocathodes as the limiting components (for enhanced arsenite/arsenate sensitivity). Figure 5 demonstrates the mediated bioelectrocatalytic oxidation of glucose by FAD-GDH, where the presence of arsenite and arsenate do not affect enzymatic activity. Figure 6A presents a polarization and resulting power curve for the glucose/O_2 EFC, in the absence and presence of arsenite/arsenate. EFCs were evaluated galvanostatically, by drawing gradually increasing current from the EFC until short circuit (ramp rate of 1 μA/s). The EFCs possessed open circuit potentials (OCPs) of 723.3 ± 4.5 mV. The maximum current and power densities were 289.7 ± 12.4 μA cm-2 and 57.2 ± 1.9 μW cm^{-2} (mean ± standard deviation, $n = 3$).

As a self-powered sensor that does not require any external energy source to operate, only 10% of the maximum current is drawn from the glucose/O_2 EFC and the potential difference is monitored as a function of time (Figure 6B and C). With 10% of the maximum current withdrawn from the biofuel cell, it can be seen that the biofuel cell retains approximately 73% of its OCP. Successive aliquots of arsenite or arsenate are injected into the electrolyte/buffer/fuel solution, which results in a decrease in potential difference of the EFC. For arsenite or arsenate at a final concentration of 1 mM to 20 mM, a decrease in the potential difference of the EFC of 20 mV is observed. To eliminate variation between each EFC, the percentage change of the initial OCP of EFC is averaged and plotted.

Differences in the inhibitory effects of arsenic for the self-powered EFC experiments and the amperometric laccase experiments are due to the experimental conditions employed (potentiostatic and galvanostatic), where galvanostatic experiments are continuously changing the potential of the bioelectrode. The continuously changing potential difference between the T1 Cu site of laccase and the electrode architecture continuously alter the catalytic turnover of the bioelectrodes and by default, alter the effects of the inhibitors at the bioelectrodes. [51]

Conclusions.

In conclusion, this article reports the enzymatic inhibition of laccase and laccase bioelectrodes (DET type) by both arsenite and arsenate, for which a mixed inhibition model (with preference towards an uncompetitive inhibition model) was determined by UV-Vis spectrophotometric assays. The laccase biocathodes were then employed within a glucose/O_2 EFC, yielding a self-powered arsenite/arsenate biosensor. The device possessed LODs of 13 μM for arsenite and 132 μM for arsenate, with sensitivities of 0.91 ± 0.07 mV/mM for arsenite and 0.98 ± 0.02 mV/mM for arsenate, capable for detection acute arsenite and arsenate poisoning.[52] Linear dynamic ranges for the EFCs were evaluated for 1 – 20 mM arsenite (R^2 = 0.9934) and 1 – 8 mM arsenate (R^2 = 0.9810). Further, the device only operated at 10% current draw of the maximum current density of the EFC.

While this conceptual study demonstrates how the inhibition of laccase and laccase bioelectrodes by arsenite and arsenate can yield a self-powered biosensor for their detection, future studies will address the suitability of this system in actual field samples as well as develop an array system to investigate the possible effect of other contaminants on the self-powered biosensor (*i.e.* fluoride). Interference from chloride is expected to minimal, because the use of anthracene as an orientation moiety has been demonstrated to be able to out-compete chloride inhibition (which acts as a competitive inhibitor).[53]

AUTHOR INFORMATION

Supporting information: Non-linear regression fits for laccase bioelectrode inhibition evaluation using ABTS as an electron mediator.

Corresponding Author

E-mail: minteer@chem.utah.edu.

Author Contributions

The manuscript was written through contributions of all authors. All authors have given approval to the final version of the manuscript.

ACKNOWLEDGMENTS

The authors thank the United States Department of Agriculture and the Army Research Office MURI (#W911NF1410263) grant for funding. RDM acknowledges funding from a Marie Curie-Skłodowska Individual Fellowship (Global) under the EU Commission's Horizon 2020 framework (project no. 654836).

REFERENCES

(1) McArthur, J.; Ravenscroft, P.; Safiulla, S.; Thirlwall, M. *Water Resour. Res.* **2001**, *37*, 109-117.
(2) Berg, M.; Stengel, C.; Trang, P. T. K.; Viet, P. H.; Sampson, M. L.; Leng, M.; Samreth, S.; Fredericks, D. *Sci. Total Environ.* **2007**, *372*, 413-425.
(3) Hughes, M. F. *Toxicol. Lett.* **2002**, *133*, 1-16.
(4) Reyes-Salas, E.; Dosal-Gomez, M.; Barcelo-Quintal, M.; Manzanilla-Cano, J. *Anal. Lett.* **2002**, *35*, 123-133.
(5) Sharma, P. *Anal. Sci.* **1995**, *11*, 261-262.
(6) Li, H.; Smart, R. B. *Anal. Chim. Acta* **1996**, *325*, 25-32.
(7) Adeloju, S.; Young, T. *Anal. Lett.* **1997**, *30*, 147-161.
(8) Tercier-Waeber, M. L.; Pei, J.; Buffle, J.; Fiaccabrino, G.; Koudelka-Hep, M.; Riccardi, G.; Confalonieri, F.; Sina, A.; Graziottin, F. *Electroanalysis* **2000**, *12*, 27-34.

(9) Nolan, M. A.; Kounaves, S. P. *Anal. Chem.* **1999**, *71*, 3567-3573.
(10) Sekretaryova, A. N.; Beni, V.; Eriksson, M.; Karyakin, A. A.; Turner, A. P.; Vagin, M. Y. *Anal. Chem.* **2014**, *86*, 9540-9547.
(11) Li, Z.; Rosenbaum, M. A.; Venkataraman, A.; Tam, T. K.; Katz, E.; Angenent, L. T. *Chem. Commun.* **2011**, *47*, 3060-3062.
(12) Zhou, M.; Zhou, N.; Kuralay, F.; Windmiller, J.; Parkhomovsky, S.; Valdes-Ramirez, G.; Katz, E.; Wang, J. *Angew. Chem. Int. Ed.* **2012**, *51*, 2686-2689.
(13) Cheng, J.; Han, Y.; Deng, L.; Guo, S. *Anal. Chem.* **2014**, *86*, 11782-11788.
(14) Sekretaryova, A. N.; Beni, V.; Eriksson, M.; Karyakin, A. A.; Turner, A. P. F.; Vagin, M. Y. *Anal. Chem.* **2014**, *86*, 9540-9547.
(15) Hou, C.; Fan, S.; Lang, Q.; Liu, A. *Anal. Chem.* **2015**, *87*, 3382-3387.
(16) Pinyou, P.; Conzuelo, F.; Sliozberg, K.; Vivekananthan, J.; Contin, A.; Pöller, S.; Plumeré, N.; Schuhmann, W. *Bioelectrochemistry* **2015**, *106, Part A*, 22-27.
(17) Zhou, M. *Electroanalysis* **2015**, *27*, 1786-1810.
(18) Kang, Z.; Gu, Y.; Yan, X.; Bai, Z.; Liu, Y.; Liu, S.; Zhang, X.; Zhang, Z.; Zhang, X.; Zhang, Y. *Biosens. Bioelectron.* **2015**, *64*, 499-504.
(19) Strambini, L. M.; Longo, A.; Scarano, S.; Prescimone, T.; Palchetti, I.; Minunni, M.; Giannessi, D.; Barillaro, G. *Biosens. Bioelectron.* **2015**, *66*, 162-168.
(20) Zhao, Y.; Fu, Y.; Wang, P.; Xing, L.; Xue, X. *Nanoscale* **2015**, *7*, 1904-1911.
(21) Jia, X.; Dong, S.; Wang, E. *Biosens. Bioelectron.* **2016**, *76*, 80-90.
(22) Sode, K.; Yamazaki, T.; Lee, I.; Hanashi, T.; Tsugawa, W. *Biosens. Bioelectron.* **2016**, *76*, 20-28.
(23) Zhang, L.; Zhou, M.; Dong, S. *Anal. Chem.* **2012**, *84*, 10345-10349.
(24) Wen, D.; Deng, L.; Guo, S.; Dong, S. *Anal. Chem.* **2011**, *83*, 3968-3972.
(25) Conzuelo, F.; Vivekananthan, J.; Pöller, S.; Pingarrón, J. M.; Schuhmann, W. *ChemElectroChem* **2014**, *1*, 1854-1858.
(26) Deng, L.; Chen, C.; Zhou, M.; Guo, S.; Wang, E.; Dong, S. *Anal. Chem.* **2010**, *82*, 4283-4287.
(27) Wen, D.; Deng, L.; Guo, S.; Dong, S. *Anal. Chem.* **2011**, *83*, 3968-3972.
(28) Deng, L.; Chen, C.; Zhou, M.; Guo, S.; Wang, E.; Dong, S. *Anal. Chem.* **2010**, *82*, 4283-4287.
(29) Sakai, H.; Nakagawa, T.; Tokita, Y.; Hatazawa, T.; Ikeda, T.; Tsujimura, S.; Kano, K. *Energy Environ. Sci.* **2009**, *2*, 133-138.
(30) Cinquin, P.; Gondran, C.; Giroud, F.; Mazabrard, S.; Pellissier, A.; Boucher, F.; Alcaraz, J. P.; Gorgy, K.; Lenouvel, F.; Mathe, S.; Porcu, P.; Cosnier, S. *PLoS One* **2010**, *5*, 1 - 7.
(31) Mano, N.; Mao, F.; Heller, A. *J. Am. Chem. Soc.* **2003**, *125*, 6588-6594.
(32) Meredith, M. T.; Minteer, S. D. *Anal. Chem.* **2011**, *83*, 5436-5441.
(33) Katz, E.; Bückmann, A. F.; Willner, I. *J. Am. Chem. Soc.* **2001**, *123*, 10752-10753.
(34) Newman, J. D.; Turner, A. P. *Biosens. Bioelectron.* **2005**, *20*, 2435-2453.
(35) Barrière, F.; Kavanagh, P.; Leech, D. *Electrochim. Acta* **2006**, *51*, 5187-5192.
(36) Brunel, L.; Denele, J.; Servat, K.; Kokoh, K. B.; Jolivalt, C.; Innocent, C.; Cretin, M.; Rolland, M.; Tingry, S. *Electrochem. Commun.* **2007**, *9*, 331-336.
(37) Mano, N.; Mao, F.; Heller, A. *J. Am. Chem. Soc.* **2003**, *125*, 6588-6594.
(38) Barrière, F.; Ferry, Y.; Rochefort, D.; Leech, D. *Electrochem. Commun.* **2004**, *6*, 237-241.
(39) Scodeller, P.; Carballo, R.; Szamocki, R.; Levin, L.; Forchiassin, F.; Calvo, E. J. *J. Am. Chem. Soc.* **2010**, *132*, 11132-11140.
(40) Gallaway, J. W.; Barton, S. A. C. *J. Electroanal. Chem.* **2009**, *626*, 149-155.
(41) Meredith, M. T.; Minson, M.; Hickey, D.; Artyushkova, K.; Glatzhofer, D. T.; Minteer, S. D. *ACS Catal.* **2011**, *1*, 1683-1690.
(42) Milton, R. D.; Lim, K.; Hickey, D. P.; Minteer, S. D. *Bioelectrochemistry* **2015**, *106, Part A*, 56-63.
(43) Milton, R. D.; Minteer, S. D. *J. Electrochem. Soc.* **2014**, *161*, H3011-H3014.
(44) Shleev, S.; Jarosz-Wilkolazka, A.; Khalunina, A.; Morozova, O.; Yaropolov, A.; Ruzgas, T.; Gorton, L. *Bioelectrochemistry* **2005**, *67*, 115-124.
(45) Shleev, S.; Tkac, J.; Christenson, A.; Ruzgas, T.; Yaropolov, A. I.; Whittaker, J. W.; Gorton, L. *Biosens. Bioelectron.* **2005**, *20*, 2517-2554.
(46) Kuznetsov, B.; Shumakovich, G.; Koroleva, O.; Yaropolov, A. *Biosens. Bioelectron.* **2001**, *16*, 73-84.
(47) Riva, S. *Trends Biotechnol.* **2006**, *24*, 219-226.
(48) Meredith, M. T.; Minson, M.; Hickey, D.; Artyushkova, K.; Glatzhofer, D. T.; Minteer, S. D. *ACS Catal.* **2011**, *1*, 1683-1690.
(49) Cornish-Bowden, A. *Biochem. J.* **1974**, *137*, 143.
(50) Lineweaver, H.; Burk, D. *J. Am. Chem. Soc.* **1934**, *56*, 658-666.
(51) Amine, A.; Alafandy, M.; Kauffmann, J.-M.; Pekli, M. N. *Anal. Chem.* **1995**, *67*, 2822-2827.
(52) Ratnaike, R. N. *Postgrad. Med. J.* **2003**, *79*, 391-396.
(53) Milton, R. D.; Giroud, F.; Thumser, A. E.; Minteer, S. D.; Slade, R. C. T. *Chem. Commun.* **2014**, *50*, 94-96.

For TOC only

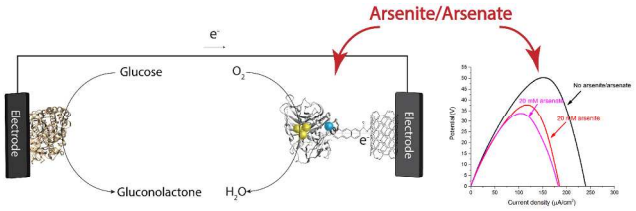
Arsenite/Arsenate
e⁻
Glucose
O2
Electrode
Electrode
Gluconolactone
H2O
e⁻
No arsenite/arsenate
20 mM arsenite
20 mM arsenite
Potential (V)
Current density (uA/cm²)